

# NORMAL TISSUE COMPLICATION PROBABILITY MODELS

Gian Marco Miccio (10768466),  
Gianluca Villa (10709798),  
Stefano Zara (10730272)

in collaboration with:

Dr. Tiziana Rancati, Alessandra Catalano, Alessandro Cicchetti

February 2025

## 1 Introduction

The choice of topic for this project in the Nonparametric Statistics course was heavily influenced by our previous work on last year's project for the Applied Statistics course. The dataset we have chosen for this analysis is, in fact, the same one we previously examined. We would like to extend our deepest gratitude to our tutors, whose guidance, assistance, and advice throughout both projects have been invaluable. We are particularly thankful for the opportunity to continue working with these important datasets as we take on this new challenge.

The data comes from the REQUITE project, a significant milestone in cancer research. This project has meticulously compiled patient profiles, resulting in an invaluable dataset that will support future advancements in the field.

In particular, the rare opportunity to work with dosimetric maps was the primary motivation that made us excited about continuing with this project. Further in this report, we will provide a more detailed explanation of what these maps are and how they work. The academic courses we had attended previously did not offer formal training on how to properly handle image data, so we were eager to gain new insights from this experience. Additionally, the sense of pride and responsibility associated with working in the medical field provided an added boost of motivation.

As the project progressed throughout last year, our interest grew stronger. By the time we submitted and presented our results for the Applied Statistics course, we felt that our work was not yet complete. The results obtained using parametric methods alone lacked a broader perspective, especially in relation to the maps. Thus, we were eager to explore the datasets with new nonparametric tools.

From feature selection to survival analysis (a common tool for medical datasets), the nonparametric algorithms introduced in this course proved to be particularly useful in furthering our understanding of the dataset we were working with.

Despite the careful consideration required when working in the medical field, there is a possibility that our results might be used by other researchers. If that happens, we would be greatly honored. The thought that some of the insights from our work might be considered by oncologists when planning radiation doses for patients in the radiotherapy process would be a tangible contribution for which we would be incredibly proud. As we have observed, many ongoing studies in this area utilize a variety of techniques to analyze dosimetric maps. This is due to the increasing challenge and necessity of customizing radiation intensity and shape on a patient-level basis, with the aim of designing radiotherapy treatments tailored to individual patient characteristics as technological advancements continue.

Ultimately, this project aims to offer a new perspective on the analysis of dosimetric maps for prostate cancer patients undergoing radiotherapy, with its novelty lying in the application of nonparametric tests directly on the maps.

## 2 General overview

Together with prostatectomy (the removal of the prostate), radiotherapy is one of the main techniques used to treat prostate cancer. In some cases, these two treatments are combined, with radiotherapy administered either after prostatectomy to eliminate any remaining cancer cells or, less commonly, before surgery to shrink the tumor. Despite benefiting from technological advancements in recent years, radiotherapy can still result in unwanted side effects. Most of these side effects are related to damage to nearby organs, such as the bladder and rectum, as they are in close proximity to the prostate and are therefore more likely to be affected by radiation. For instance, urinary incontinence, erectile dysfunction, and bowel dysfunction are among the common comorbidities associated with this treatment.

It is relatively easy to assess how many of these side effects actually occurred in the sample, and the number is quite significant. This is partly due to the elderly population selected; however, it cannot be ignored how much these complications can hinder a patient's quality of life. Therefore, they are worth studying and trying to predict, with the goal of improving the patient's overall well-being.

## 3 Aim

For each of these side effects, our objective is to identify which clinical data and map characteristics contribute the most to their occurrence, using techniques such as survival models. In particular, after building Cox models for the selected side effects and proposing a new strategy to analyze the maps, we were pleased

to see that the results of the survival analysis were consistent with the findings in the maps.

## 4 Dataset description

In this section, we will briefly describe our dataset and some pre-processing steps that we applied.

### 4.1 Side effects

As previously explained, side effects were the target variables for this project. More specifically, we had access to the level of toxicity (ranging from 0 = no toxicity to 4 = severe condition) for each side effect at each endpoint: baseline level, level after 1 month, level for each subsequent visit, every 6 months.

To ensure that we were only analyzing the side effects due to radiotherapy, we applied the following transformation:

$$\text{level}(T_j) = \begin{cases} \text{level}(T_j) & \text{if } \text{level}(T_j) > \text{level}(T_0) \\ 0 & \text{else} \end{cases} \quad \forall T_j = 1 \text{ month}, 6 \text{ months}, 1 \text{ year}, \dots$$

In this way, patients for whom the level of a side effect remained unchanged (or, in rare cases, decreased) following radiotherapy are assigned a level of 0, as radiotherapy did not exacerbate the patient's condition.

### 4.2 Clinical features

For each patient, we had access to a range of clinical features, including information about the patient's habits (such as whether they are a smoker or consume alcohol), pre-existing complications (such as diabetes and hypertension), details regarding how the radiotherapy was administered, any possible additional interventions (e.g., TURP - Transurethral Resection of the Prostate), as well as information on pelvic treatment and whether the patient had undergone prostatectomy (removal of the prostate).

### 4.3 Dosimetric maps

The dosimetric maps are a central component of the project, providing a unique type of data. Initially, the dosimetric maps for both the rectum and bladder are three-dimensional (3D) datasets, where each voxel (volume element) represents a specific region within the organs and encodes the radiation dose received at that point. These 3D maps were then processed to generate two-dimensional data, ensuring uniform spatial dimensions across all maps, resulting in what are known as normalized dosimetric maps.

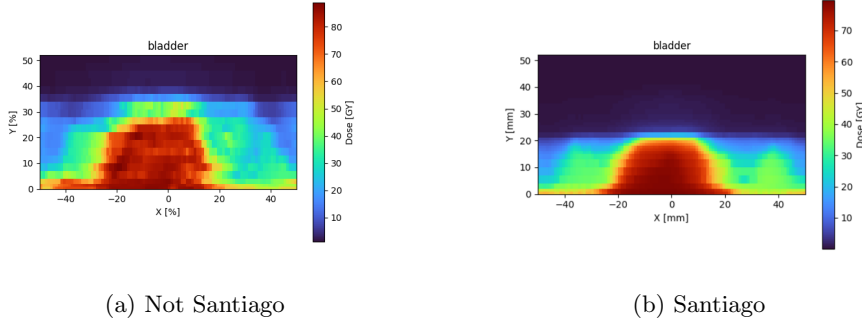


Figure 1: Example of two different patients' maps. The one from Santiago has a more regular shape due to the radiotherapy technique adopted.

The radiation intensity is measured in grays, ranging from 0 to a maximum near 80 grays. Normalized maps tend to have bands of radiation of the same intensity in the lowest and highest rows as this is a consequence of the stretching of the map the normalization procedure inevitably introduces. In addition, every hospitalization site has its own technique of radiotherapy. The most prominent one is that of Santiago. In fact, for what regards the doses received by the bladder, Santiago patients show a more geometric pattern, due to the old and obsolete procedure of masking the X-ray machines generator with some basic shapes

One of the first steps in dealing with these maps was to apply a smoothing technique to them. By applying the nonparametric technique of penalized splines, that allows to reduce noise in the image while still preserving their original shape and trends. An example of the result of smoothing can be seen in figure 2.

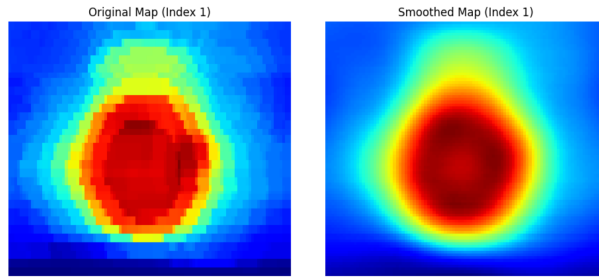


Figure 2: Example of a map of the rectum pre and post smoothing

An important observation must be made on the dataset and the way it was divided, as it turned out to be pivotal for the entire analysis.

Prostatectomy is a binary variable in the dataset that refers to whether or not a patient has undergone the surgical procedure of prostate gland removal,

which affects completely not only the internal anatomy of the human body in the area of interest for the radiation therapy, but also the way the therapy is approached in the first place.

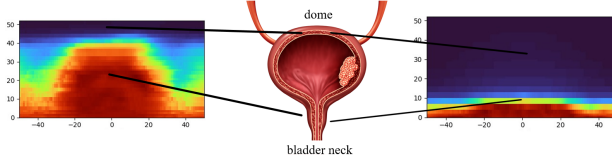


Figure 3: on the left a dosimetric map of a patient that has not undergone prostatectomy, on the right the one of a patient that has

As shown in figure 3, the dosimetrics maps change drastically depending on whether or not the patient has undergone prostatectomy, and for this reason they must be treated separately in the analysis. It is important to notice how different dosimetric maps affect differently the possible side effects that a patient might suffer from. Irradiating the bladder neck like in the example of the patient that has not undergone prostatectomy, will naturally result in a higher probability of urinary related side effects.

Other variables of equal importance have been identified in TURP and pelvic treatments.

The first one refers to the surgical practice of Transurethral Resection of the Prostate, a minimally invasive procedure performed without any external incision, through the urinary cavity, to remove a portion of the prostate gland in case of urine flow obstruction. Though not of curative effect, it can be undergone to relieve the patient of some urinary related symptoms, and thus affects the outcome of some of the side effects that are of interest in the study.

The second one refers instead to the treatments involving the pelvic structure, which not only includes the prostate, main interest of the treatment, but also the surrounding organs and structures, like pelvic lymph nodes and the rectum. These treatments could include Pelvic Lymph Node Dissection (PLND) and any other surgery that alters the anatomical structure of this part of the body. Patients undergoing this type of radiotherapy will not only have different radiation plans and maps to begin with, but may also present different side effects with different rates.

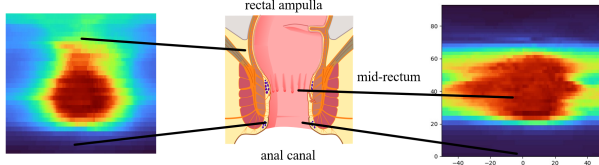


Figure 4: On the left, the dosimetric maps on the rectum of a patient that has not undergone a pelvic treatment, on the right the one of a patient that has

Notice in figure 4 the difference in the radiation maps for the rectum in patients that have undergone pelvic treatments. Same argument as prostatectomy, this would affect the analysis if not treated separately.

## 5 FPCA Scores

To include images as features in our dataset, we decided to compute numerical indexes to characterize the doses distributions for each map. Our method consists of applying Functional Principal Component Analysis (FPCA) to the dosimetric maps and using the resulting scores as indexes to represent the dose distributions. For this study, we used three principal components, obtaining three numerical indexes to represent each map. To interpret the physical meaning of these scores, we can visualize the corresponding principal axes:

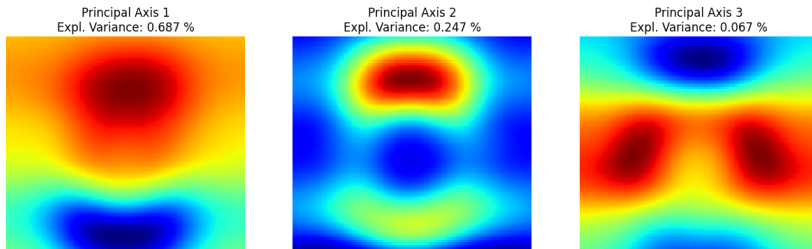


Figure 5: Principal axes for rectum maps of patients that didn't go under pelvic treatment. These maps should not be interpreted as dosimetric maps, but they are highly useful for understanding the meaning of the principal components. For example, a high value of the first principal component indicates that the doses are more concentrated in the upper part, and less concentrated in the lower part, compared to the mean.

**Note:** The subdivision of rectum and bladder maps based on prostatectomy and pelvic treatments is crucial when using FPCA-derived indexes. In fact, if FPCA were applied without this subdivision, we would obtain the following results:

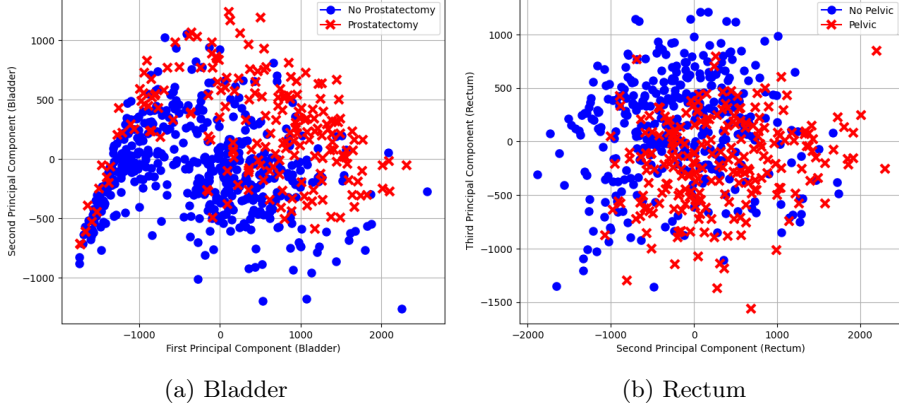


Figure 6: FPCA scores without subdivision by prostatectomy/pelvic factors

As shown in the plot, the FPCA scores of bladder and rectum strongly correlate with the pelvic and prostatectomy factors respectively, making the analysis biased towards these factors.

## 6 P-value maps

We thought information carried by the maps could be further exploited to identify which pixels within a map are most meaningful for each endpoint. Therefore, in this section, we propose an approach to examine the relationship between the presence of side effects and dosimetric maps that relies on non-parametric tests.

Firstly, we applied P-splines **smoothing** and **downsampling** techniques to the maps, by averaging the pixels in a neighborhood of size 2. The purpose of these operations is not only to remove noise but also to make the analysis less "local". In fact, both smoothing and downsampling are processes that depend on the neighborhood of a pixel. As a result, the value of a pixel in the processed maps reflects the characteristics of its surrounding neighborhood in the original map. An additional advantage of these preprocessing techniques is that they are likely to yield more interpretable results, and downsampling also reduces computational complexity.

### 6.1 Difference Map

Suppose fixing a side effect, and divide the patients maps in two groups:  $\mathbf{M}^0$  represents the maps of patients who did not experience the considered side effect, and  $\mathbf{M}^1$  represents the maps of those who did. The first step involves calculating the **pixel-wise mean map** for the two groups and to retrieve their difference. To ensure that our analysis is robust with respect to outliers, we use the trimmed mean instead of the sample mean. Computing the trimmed mean

of a vector means computing the mean by excluding the 10% most extreme values.

Therefore, we compute the **difference map**  $D$  as follows:

$$D_{ij} = \text{trimmean}(\mathbf{M}_{ij}^1) - \text{trimmean}(\mathbf{M}_{ij}^0), \quad \forall i, j \quad (1)$$

where  $\mathbf{M}_{ij}^0$  represents the vector of values (in Grays) for the maps in  $\mathbf{M}^0$  at location  $i, j$  and  $\mathbf{M}_{ij}^1$  corresponds to the values in  $\mathbf{M}^1$ . This resulting map provides insight into the regions exhibiting the greatest mean differences between the two groups. However, a critical question remains: how can we determine if these differences are statistically significant?

## 6.2 Statistical Significance

To determine if the differences in  $D$  are statistically significant, we compute a map  $P$ , of the same size of  $D$ , where the  $(i, j)$ -th entry of  $P$  is the **p-value** of the following test:

$$H_0 : \mathbf{M}_{ij}^0 \stackrel{d}{=} \mathbf{M}_{ij}^1 \quad \text{vs} \quad H_1 : \mathbf{M}_{ij}^0 \stackrel{d}{<} \mathbf{M}_{ij}^1 \quad (2)$$

We will refer to  $P$  as the **p-values map**.

Since the distribution of each pixel can be irregular, to avoid relying on any particular assumption, we computed the p-values using **permutational tests**, using the trimmed mean as test statistic.

To account for class imbalance, we performed several permutation tests for each pixel by resampling the class with the higher numerosity. Assuming group 0 is the majority group, with  $n_0$  and  $n_1$  representing the group sizes, we defined:

$$n'_0 = \min(1, 2 \cdot \frac{n_1}{n_0}) \cdot n_0 \quad (3)$$

and computed the permutational test using only  $n'_0$  data points from  $\mathbf{M}_{ij}^0$ , sampled at random. We repeated this process  $10 \cdot \lceil n_0/n_1 \rceil$  times to obtain robust results.

## 6.3 Weighting Function and Combined Map

Now, we aim to identify the pixels for which the difference in dose distribution is sufficiently **large** (greater than or approximately equal to 5 Grays) and **statistically significant** (with p-values  $< 0.05$ ). Although the two maps are not independent, we can still interpret the results by **combining the informations from  $D$  and  $P$** . A simple way to do this is by directly multiplying (pixel-wise) the difference map by a transformation of the p-values map. We want this transformation to be positive in the range  $[0, 1]$  and monotonically decreasing, in order to give higher weight to smaller p-values. We would also like to be able to fix a proper significance level  $\alpha$ .

Specifically, for p-values less than alpha, we want a function that decreases slowly, as all p-values below alpha are significant for us. For p-values greater

than alpha, we want a function that decreases rapidly. The function is defined as:

$$W_{i,j} = W(p_{i,j}) = \begin{cases} 1 - k \cdot p_{i,j}^2, & 0 \leq p_{i,j} \leq \alpha \\ A(e^{-b \cdot (p_{i,j}-1)} - 1), & \alpha < p_{i,j} \leq 1 \end{cases} \quad \forall i, j \quad (4)$$

where  $k, b > 0$ , and

$$A = \frac{1 - k \cdot \alpha^2}{e^{-b \cdot (\alpha-1)} - 1} \quad (5)$$

ensures that  $W$  is continuous in  $\alpha$ . The parameter  $k$  tunes the slope of the function for  $p_{i,j} \leq \alpha$ , and the parameter  $b$  adjusts the slope for  $p_{i,j} > \alpha$ .

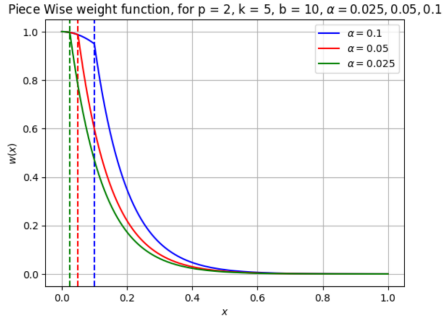


Figure 7: Weight function

For our studies, we set  $k = 5, b = 10$ , and  $\alpha = 0.05$ .

Once the matrix  $W$  is obtained, we compute the **combined map**  $C$  as:

$$C_{ij} = D_{ij} \cdot W_{ij} \quad \forall i, j \quad (6)$$

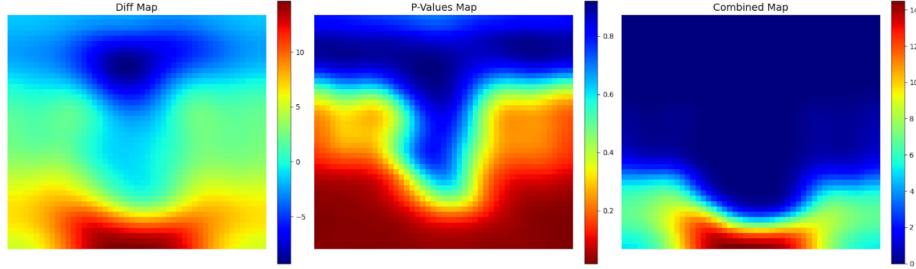
## 6.4 Results

In this section, we present the results obtained by applying this method to our data. As described earlier, we categorized our patients into two groups based on bladder involvement: one group consisting of patients who underwent prostatectomy and another group consisting of those who did not. Similarly, we divided the patients into two groups based on rectal involvement: one group receiving pelvic radiotherapy and another group not receiving pelvic radiotherapy.

In the following examples, we will plot difference maps, p-value maps, and combined maps for the considered side effects, and we will provide an interpretation of the obtained results, drawing on clinical literature.

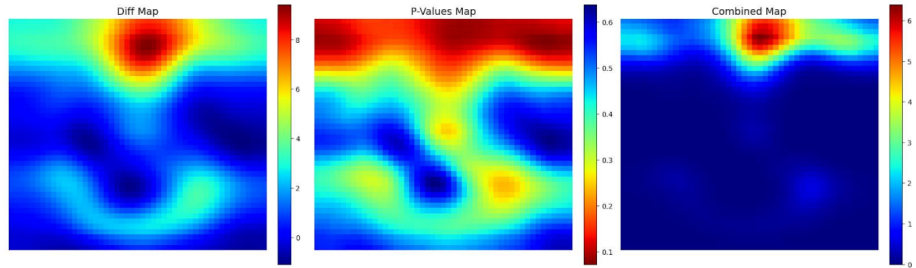
### 6.4.1 Management of Sphincter Control (No Pelvic Radiotherapy)

In this analysis, the dataset was highly imbalanced ( $n_0 = 330, n_1 = 36$ ). Following the previously outlined method, we performed 100 bootstrap iterations by resampling  $n'_0 = 72$  data points from group 0.



The results are promising: on average, the doses are higher for patients who experienced this side effect in both the **lower and central regions**. However, the p-value map reveals that the differences in the central region are not statistically significant, with p-values around 0.3. In contrast, the differences in the lower region are highly significant, with p-values  $< 0.1$  across the entire lower region and  $< 0.05$  in the bottom left and bottom right areas. These regions exhibit the most significant statistical differences, but the average dose difference is not particularly high ( $\sim 5$  Grays), so they do not have the highest impact on the combined map. Our method correctly identifies the lower region as the most significant, as this region corresponds to the distal (inferior) rectum, which is anatomically closer to the anal canal and sphincter area. This region is critical for functions related to sphincter control and may be more susceptible to radiation induced side effects such as fecal incontinence or difficulties in bowel regulation. Furthermore, irradiation of the lower lateral regions is likely to affect nerve function, potentially leading to sensory deficits and reduced coordination of sphincter activity.

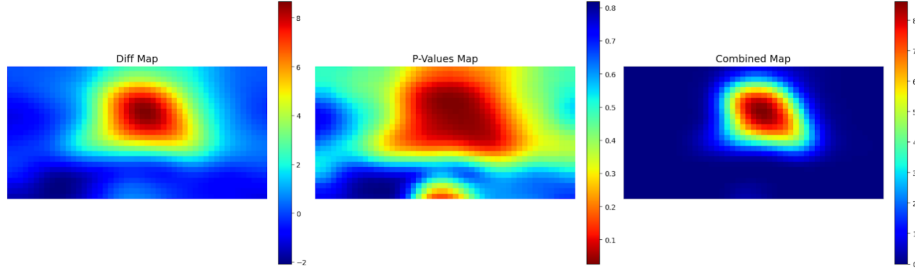
#### 6.4.2 Diarrhoea (No Pelvic Radiotherapy)



Similarly, the data was highly unbalanced in this case: ( $n_0 = 340, n_1 = 26$ ). The difference map also identified the central region as potentially sensitive. However, the p-values in this region were not statistically significant, leading to its exclusion from the combined map. As a result, the upper region emerged

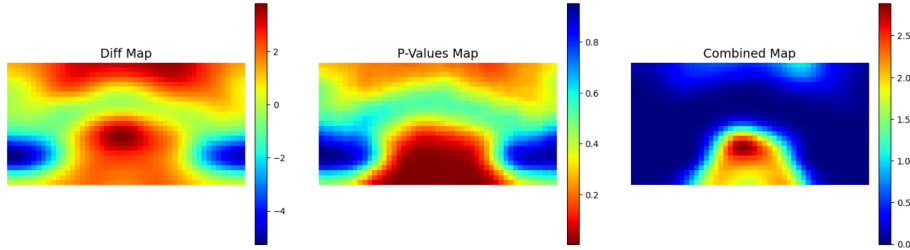
as the most sensitive, which is consistent with its anatomical proximity to the intestinal region.

#### 6.4.3 Urinary Incontinence (No Prostatectomy), for endpoints in 1-2 years



The upper-central part of the bladder is located near the bladder neck and the periurethral area, both of which are crucial for urinary function. Irradiation in these areas can damage the muscles and nerves responsible for urine retention, potentially leading to symptoms such as incontinence, urgency, and frequency. In general, chronic urinary symptoms are more often associated with irradiation of the central-upper region. As we will discuss in the following sections, these results are strongly supported by the use of the Functional PCA indices in the Survival Analysis models.

#### 6.4.4 Urinary Incontinence (Prostatectomy)



The difference map does not provide significant insight, as it indicates that the doses for patients with urinary incontinence are, on average, higher across the lower, central, and upper regions. However, by examining the p-value map, we observe that the p-values in the upper region are not statistically significant ( $\sim 0.3$ ), while those in the lower region are less than 0.1. By observing the combined map, we conclude that only the lower region receives significantly higher doses in patients with urinary incontinence.

This finding is consistent with anatomical and functional considerations: the lower region corresponds to the bladder neck, which plays a crucial role in both the storage and release of urine. The bladder neck contains the internal urethral sphincter, a smooth muscle ring that remains contracted to prevent involuntary urine leakage, relaxing only during urination. Radiation exposure to this area can lead to fibrosis and nerve damage, weakening sphincter function and impairing urine retention. After prostatectomy, the bladder neck becomes even more critical, as the removal of the prostate alters the anatomy and affects the external sphincter. Patients must rely more heavily on the bladder neck to maintain continence, making it highly vulnerable to radiation-induced dysfunction. Damage to this region can lead to persistent urinary incontinence, as the primary continence mechanism postsurgery is compromised.

It is important to note that in the combined map, the dose differences are relatively small—only 2.5 "Equivalent Grays." While the differences are statistically significant, they are not large, indicating that the impact may not be as pronounced. This also serves as a useful interpretation for unexpected results: if all regions show low values in the combined map (e.g., below 1), it suggests that the results should be interpreted with caution.

## 7 Survival Analysis

We use proportional Cox models to investigate the relationship between the time elapsed before the onset of a side effect and the FPCA indices derived from the maps. Specifically, we considered only time points beyond one year and used only the indices related to bladder maps for urinary symptoms and rectal maps for rectal symptoms. Separate models were built based on the subdivision of patients according to pelvic treatment and prostatectomy factors. Additionally, clinical data were incorporated into the models, and the site of origin was included as a random effect.

To account for the different severity levels of symptoms, observations corresponding to side effect levels greater than 2 were duplicated as many times as their severity level, thereby assigning them greater weight in the analysis.

### 7.0.1 Comparison with p-Value Maps

The agreement between survival analysis results and permutational p-value maps is not necessarily expected, as the two approaches answer different questions. Survival analysis addresses a temporal aspect, determining how influential a feature is in the time-to-event of an endpoint and in which direction. In contrast, p-value maps do not account for time but instead highlight the most relevant regions of a dosimetric map.

However, we were pleased to find that many of the models we built identified FPCA indices as influential in ways that align with the areas highlighted by the p-value maps, particularly when considering endpoints at 1–2 years.

## 7.1 Remarkable results

### 7.1.1 Urinary Incontinence, no prostatectomy

The most striking result we observed was the Cox model for urinary incontinence in patients who had not undergone prostatectomy.

This model identified the **third FPCA score** as a protective factor, as indicated by its **negative coefficient**.

To verify whether this result was consistent with our findings from the p-value map analysis, we conducted a comparison, leading to the following observations:

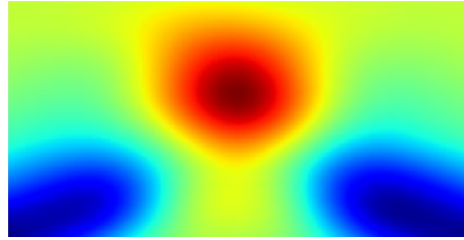


Figure 8: Plot of the third principal axis, with **sign inverted**. The plot illustrates that a negative value of the third FPCA score corresponds to dose distributions that are concentrated toward the upper central region of the patient maps.

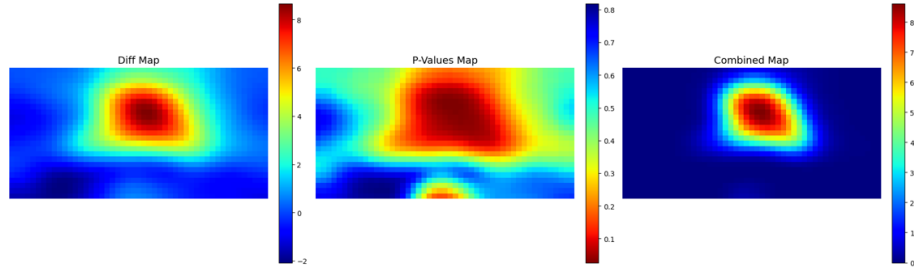


Figure 9: These are the difference, p-value, and combined maps for urinary incontinence toxicity that we discussed in the previous section, considering only endpoints at 1–2 years. As said before, the central-upper region of the map emerges as the most significant. The lateral and lower-central regions also exhibit low p-values, but due to their low mean differences, they are not prominently represented in the combined map.

The upper-central part of the bladder map, for patients that did not undergo prostatectomy, is located near the bladder neck and the periurethral area, both of which are crucial for urinary function. Irradiation in these areas can damage

the muscles and nerves responsible for urine retention, potentially leading to symptoms such as incontinence, urgency, and frequency.

In this Cox model, several clinical features also appeared: age (with a positive coefficient), smoking status (also with a positive coefficient), and TURP (transurethral resection of the prostate, which is the most common surgical technique used to remove obstructions in the bladder, with a positive coefficient).

What truly excited us about this result was the agreement between the two methods we used. The consistent findings across both approaches provided stronger evidence regarding which bladder regions are most sensitive to radiation in the onset of urinary incontinence, and further validated the effectiveness of the FPCA scoring system we developed.

### 7.1.2 Proctitis, pelvic treatment

Another remarkable survival model was the one addressing proctitis in patients who had undergone pelvic treatment.

In the output, we observed a positive coefficient for the **second FPCA component**.

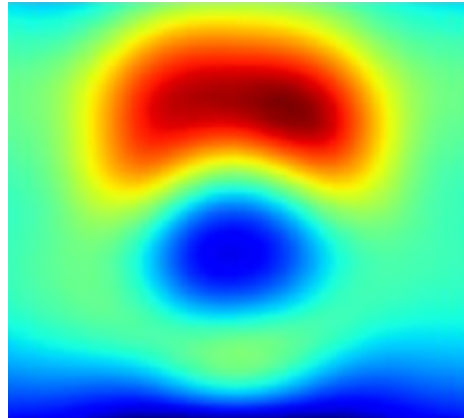


Figure 10: Plot of the second principal axis. As with the previous analysis, a positive value of the second FPCA score indicates that the doses tend to be located more toward the upper-central region of the patient's maps, relative to the mean.

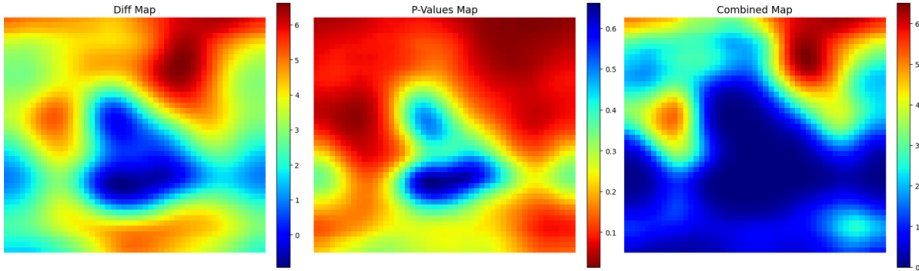


Figure 11: Here, the p-value and combined maps appear more noisy compared to the previous analysis. However, it is clear that the region identified as most significant is the upper area, where all p-values are below 0.1. In contrast, doses in the central and lower regions are less important.

Regarding the clinical features that appeared in this model, we found a negative effect (indicating a positive coefficient) for both diabetes and alcohol intake.

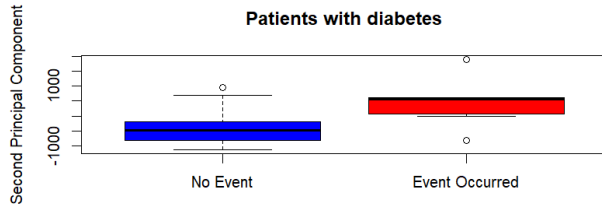


Figure 12: Particularly remarkable is the clear separation shown in the boxplot of the **second FPCA score for patients with diabetes**: there is no intersection in the interquartile ranges (IQRs).

### 7.1.3 Management of sphincter control, pelvic treatment

The last case we'd like to present is one where two fPCA indices appear simultaneously. How should we interpret such a case? We are modeling the management of sphincter control in patients with pelvic treatment, and we found that both the second and third principal components are significant, with a positive coefficient.

Despite PCA scores being numerically uncorrelated, what happens if we look at their image representation?

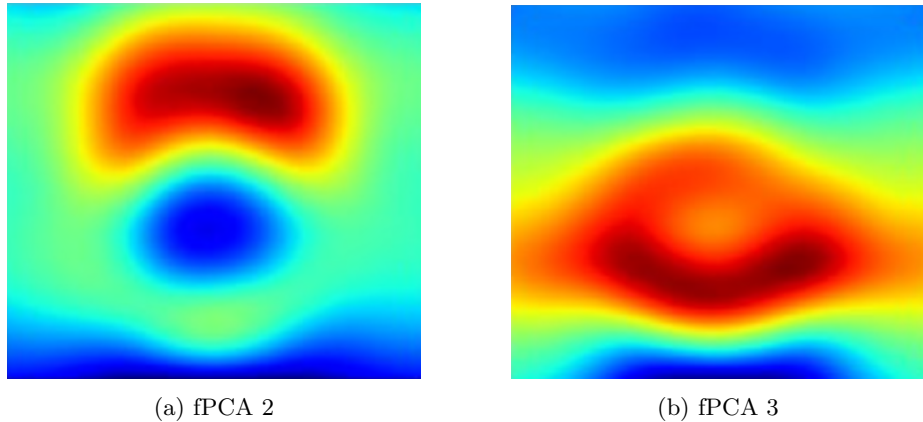


Figure 13: This are the second and the third functional principal axes. One should notice that in the central part of the maps the two principal axes have an opposite sign. So, how to interpret their combination?

A possible way to interpret the combined effect of two principal component is to plot the map which corresponds to a linear combination of the two principal axes, using as weights the coefficients obtained in the Cox model (which in this case were really similar).

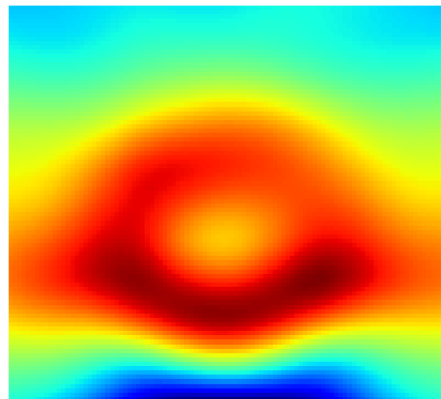


Figure 14: Plot of a linear combination of the two axes, we observe that doses in the central region, particularly the lower-central area, appear to be the most important.

For clarity, here's an example with five patients and their rectum dosimetric maps, presented in ascending order of the second and third principal component values, following the bisector.

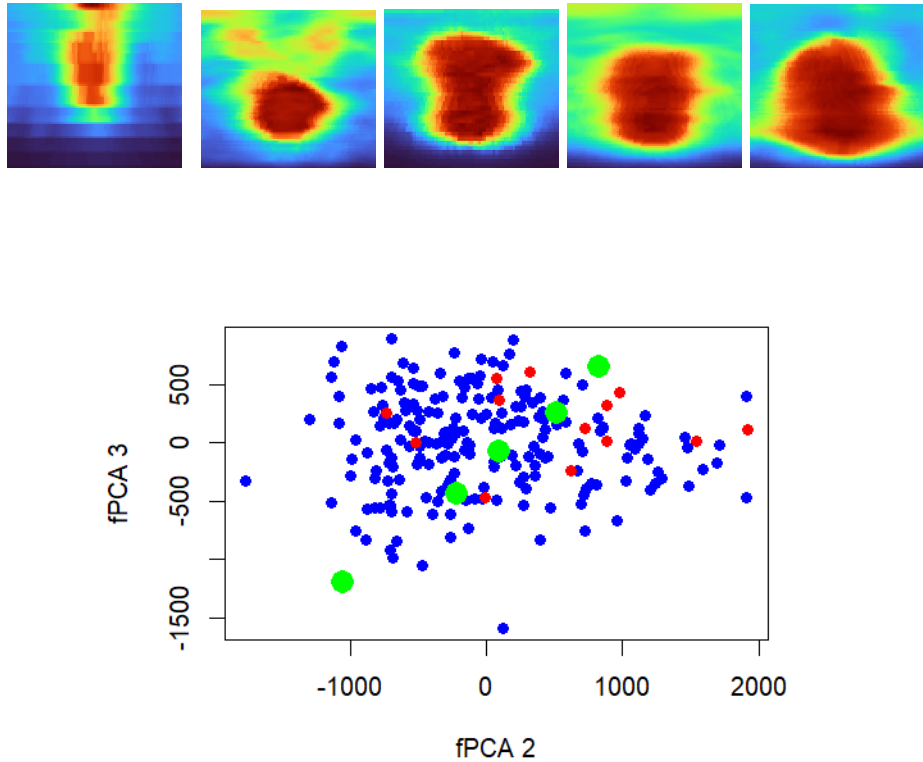


Figure 15: As we move to the right, the second and third fPCA scores increase, and, as expected, the doses shift towards the lower and lateral regions, which are the most influential zones for the management of sphincter control endpoint, according to the previous analysis. The patients in this example are denoted by green dots, ordered from bottom-left to top-right, while the red dots represent the patients who experienced this side effect. Note that the right-most patient is the only one of the five to have the management of sphincter control comorbidity.

What happens if we plot the pvalue maps?

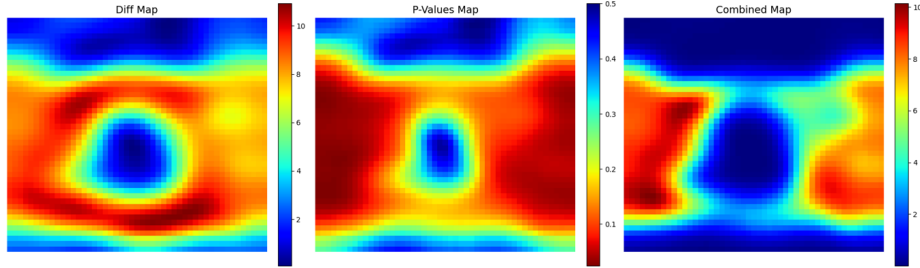


Figure 16: From the p-value maps method, we see that the lateral regions should be the most significant, therefore the central region should not be significant.

Here, we observe a discrepancy between the two methods. It's important to note that p-value maps do not account for the time factor, which could explain this difference. Lateral regions may be more prone to acute symptoms shortly after treatment, whereas central regions are associated with long-term, chronic complications.

## 8 References

- <https://www.centerforurologiccare.com/patient-education/bladder-cancer>
- <https://anatomytool.org/content/jmarchn-drawing-human-anus-no-labels>
- <https://fdapy.readthedocs.io/en/latest/>